Mon. Not. R. Astron. Soc. **000**, 1–?? (2014) Printed 20 November 2014 (MN LATEX style file v2.2)

A glitch and an anti–glitch in the anomalous X-ray pulsar 1E 1841-045

S. Şaşmaz Muş[1⋆], Berk Aydın[1], and Ersin Göğüş[1]
[1] *Sabancı University, Orhanlı- Tuzla, İstanbul, 34956, Turkey*

arXiv:1411.5274v1 [astro-ph.HE] 19 Nov 2014

20 November 2014

ABSTRACT

We investigated the long-term spin properties of the anomalous X-ray pulsar (AXP) 1E 1841-045 by performing a temporal analysis of archival *RXTE* observations spanning about 5.2 yr from 2006 September to 2011 December. We identified two peculiar timing anomalies within ∼1 yr of each other: a glitch with $\Delta\nu/\nu\sim4.8\times10^{-6}$ near MJD 54303; and an anti-glitch with $\Delta\nu/\nu\sim-5.8\times10^{-7}$ near MJD 54656. The glitch that we identified, which is the fourth glitch seen in this source in the 13 yr of RXTE monitoring, is similar to the last two detected glitches. The anti-glitch from 1E 1841-045, however, is the first to be identified. The amplitude of the anti-glitch was comparable with that recently observed in AXP 1E 2259+586. We found no significant variations in the pulsed X-ray output of the source during either the glitch or the anti-glitch. We discuss our results in relation to the standard pulsar glitch mechanisms for the glitch, and to plausible magnetospheric scenarios for the anti-glitch.

Key words: pulsars: individual (1E 1841-045) − stars: neutron − X-rays: stars

1 INTRODUCTION

Anomalous X-ray pulsars (AXPs), along with soft gamma-ray repeaters (SGRs) are extremely magnetized neutron stars (magnetars) powered by the decay of their strong magnetic fields. These sources exhibit numerous unusual characteristics, such as, relatively slow rotation speeds, high spin-down rates, bright persistent X-ray emission and, for most of them, episodic bursts seen in X-rays (see e.g., Rea & Esposito 2011; Mereghetti 2011, for recent reviews). The dipole magnetic field strengths, inferred from their spin periods and spin down rates are indeed extremely high, which are sufficient to account for their observed unique properties (Duncan & Thompson 1992).

Long term spin behaviour of magnetars usually do not follow a secular trend, likely due to large magnetic torques along with episodic wind outflow that could take place in strongly magnetized environments (Thompson et al. 2000). Additionally, sudden increase in the angular velocity (i.e., glitches) has been observed from several AXPs. However, glitch events in AXPs have peculiar differences compared to the properties of glitches from rotation powered pulsars: 1E 1048.1-5937 is one of the most variable AXP both in timing and radiative behaviour as several short energetic burst and flare events were observed (Gavriil et al. 2002; Tam et al. 2008; Dib et al. 2009; Gavriil et al. 2006). Its 2007 flare event was coincident with a large glitch (Dib et al. 2009). Similarly, AXP 4U 0142+61 went into an active period, exhibiting six bursts and a glitch event which was over-recovered, causing the neutron star to rotate slower than the pre-glitch level (Gavriil et al. 2011). Another AXP showing coincident burst and glitch event is CXOU J164710.2-455216 (Krimm et al. 2006; Israel et al. 2007b; Muno et al. 2007; Woods et al. 2011). On the other hand, 1RXS J170849.0-400910 and 1E 1841-045 have experienced glitches, but there has been no evidence of accompanying radiative enhancements in these sources (Kaspi et al. 2000; Kaspi & Gavriil 2003b; Dall'Osso et al. 2003; Israel et al. 2007a; Dib et al. 2008; Şaşmaz Muş & Göğüş 2013).

In 1E 2259+586, an outburst has been associated with a glitch (Kaspi et al. 2003a; Woods et al. 2004). More interestingly, this source exhibited a sudden decrease in its angular velocity, namely an anti-glitch (Archibald et al. 2013a), within two weeks of a hard X-ray burst (Foley et al. 2012). The sudden spin-down trend in this AXP occurred in conjunction with a doubled persistent source flux, as reported by (Archibald et al. 2013a). These authors also report that the observed anti-glitch was followed by either a glitch event ∼90 d later or by a second anti-glitch ∼50 d apart which was suggested as a more plausible explanation based on a Bayesian approach Hu et al. (2013). Unlike glitches observed from isolated neutron stars, which are generally attributed to an internal mechanism (e.g, Anderson & Itoh 1975; Alpar

⋆ E-mail: sinemsm@sabanciuniv.edu

© 2014 RAS

1977), the anti-glitch event was explained in terms of external effects, including magnetospheric processes (Lyutikov 2013; Tong 2014; Katz 2014) or the accretion of orbiting objects (Katz 2014; Ouyed et al. 2013; Huang & Geng 2013).

1E 1841-045 has a pulse period of ∼11.8 s. It is a bright persistent X-ray source with an emission spectrum extending into hard X-rays, up to about 150 keV (Kuiper et al. 2004). It is also a source of several short energetic magnetar bursts (Kumar & Safi-Harb 2010; Lin et al. 2011; Collazzi et al. 2013; Pal'shin et al. 2013). Three glitches have been observed from 1E 1841-045 with amplitudes ranging from $\sim 10^{-7}$ Hz to 1.2×10^{-6} Hz (Dib et al. 2008). Note that these events were radiatively silent, i.e, there was no significant variations of the radiative behaviour of the source associated with these timing anomalies (Dib et al. 2008; Zhu & Kaspi 2010). The persistent X-ray emission of 1E 1841-045 has remained constant during the duration of energetic bursts (Lin et al. 2011; Archibald et al. 2013b).

Here, we present the results of long-term timing analysis of 1E 1841-045 using Rossi X-ray Timing Explorer (*RXTE*) observations spanning ∼5.5 years. In the following section, we introduce these *RXTE* observations and our data analysis scheme. In §3, we present the results of our detailed temporal investigations, and report on the discovery of an anti-glitch and additional glitch from this source. We then discuss our findings in §4.

2 OBSERVATIONS AND DATA PROCESSING

1E 1841-045 has been observed with *RXTE* in 279 occasions over a time span of ∼13 years from 1999 February to 2011 December[1]. Data covering the first ∼7.6 years have already been investigated by Dib et al. (2008). Here, we investigated 137 *RXTE* observations performed from 2006 September 19 to 2011 December 8 for the first time. Additionally, we also included the last 12 (2006 April 3 - 2006 September 5) *RXTE* pointings in the sample of Dib et al. (2008) in order to link our long term timing results with their extensive coverage. Exposure times of these 149 pointings were between ∼1.2 ks and ∼9.6 ks with a mean of ∼ 4.6 ks and spacing between successive pointings varied between 0.04 and 61 days with an average of 14 days.

We employed data collected with the Proportional Counter Array (PCA), that was an array of nearly identical five proportional counter units (PCUs) operated optimally in the energy range of 2−30 keV (Jahoda et al. 2006). We first filtered each observation for occasional bursts, data anomalies and instrumental rate spikes by screening their light curves in the 2-30 keV band with the 31.25 ms time resolution. We then converted the arrival times of the remaining events to the Solar system barycenter. In order to maximize the signal-to-noise ratio for timing analysis of 1E 1841-045, we selected events in the 2−11 keV energy range recorded at the top Xenon layer of each operating PCU in GoodXenon mode, as was also done by Dib et al. (2008).

[1] The complete list of *RXTE* observations as well as pointing details can be obtained from the High Energy Astrophysics Science Archive Research Center of NASA at http://heasarc.gsfc.nasa.gov.

3 DATA ANALYSIS & RESULTS

In order to undertake coherent timing analysis, we grouped all 149 observations into six segments intercepted with observational interruptions in between due to Solar constraints. In addition, we merged observations together if the time spacing between them was less than 0.1 d. In this grouping scheme, segment 0 has 12 observations which are the last *RXTE* pointings used by Dib et al. (2008). We first generated a high signal-to-noise ratio pulse profile template using a subset of observations (typically 5-6), that were performed in the beginning of each segment. We obtained the pulse profile for each observation by folding light curves with a nominal spin frequency. We then cross-correlated the pulse profiles with the template and measured their phase shifts with respect to the template. Finally, we fitted the phase shifts with a polynomial of the following form:

$$\phi(t) = \phi_0(t_0) + \nu_0(t - t_0) + \frac{1}{2}\dot{\nu_0}(t - t_0)^2 + ... \quad (1)$$

where t_0 is the epoch time. We found that all segments, except for Segment 1 and Segment 2, are fitted well with polynomials of the third order or lower. We present the results of polynomial model fits to each segment in Table 1. We note that the spin frequency and spin-down rate of Segment 0 are consistent with those reported by Dib et al. (2008). In Table 1, we also list root-mean-square (rms) fluctuations of the resulting phase residuals, which are presented in the top panel of Figure 1. A fourth-order polynomial fit to pulse arrival times in Segment 1 yields extremely large fit statistics (χ^2 of 1508.6 for a degrees of freedom (DOF) of 21; see Figure 1 top panel and Figure 2 panel b). We therefore identified this segment to search for glitch(es), as we describe in detail below.

We fitted the pulse arrival times of Segment 2 with a fourth-order polynomial but obtain unacceptable fit statistics (χ^2/DOF = 37.8/19). We note the fact that there are systematic variations of the phase residuals around MJD 54650. Higher order polynomial fit to this segment results in lower fit statistics, whereas the errors of derived spin parameters become large. For these reasons, we also investigated this segment for searching timing anomalies.

We found that arrival times of Segment 3 can be represented with a second-order polynomial, that is the lowest order we obtained among our investigation span of 5.5 yr. We also find that the frequency derivatives[2] within this segment remain constant (see the middle panel in Figure 1). For Segments 4 and 5, we obtained an adequate fit with a third-order polynomial. However, the rms phase residual fluctuations for these segments are larger than other segments, namely Segments 0 and 3. Note the important fact that energetic short duration bursts from this magnetar were observed during Segments 4 and 5, as they are denoted with vertical solid lines in Figure 1.

In order to determine whether the large fluctuations in the phase residuals of Segments 1, 2, 4 and 5 are due to a sudden change in the spin frequency of the source, we fitted phase shifts of these segments using MPFITFUN routine

[2] Frequency derivatives are obtained by fitting a second order polynomial to subset of observations of ∼2 months long

Table 1. Pulse Ephemeris of 1E 1841-045[a]

Parameters Name	Segment 0	Segment 1[b]	Segment 2[b]	Segment 3	Segment 4	Segment 5
Range (MJD)	53829 – 54076	54126 – 54431	54492 – 54807	54860 – 55168	55223 – 55538	55588– 55903
Epoch (MJD)	53823.9694	54125.967	54491.992	54860.107	55223.090	55587.871
Number of TOAs	19	26	24	22	29	24
ν (Hz)	0.084868766(5)	*0.084861458(8)*	*0.084852295(8)*	0.084843233(2)	0.084834325(4)	0.084824920(3)
$\dot{\nu}$ (10^{-13} Hz s^{-1})	−2.82(1)	*−3.92(2)*	*−2.72(2)*	−2.834(1)	−2.883(7)	−2.943(6)
$\ddot{\nu}$ (10^{-22} Hz s^{-2})	−5.6(9)	*187(4)*	*−23(4)*	–	−9.0(5)	−4.1(4)
$d^3\nu/dt^3$ (10^{-28} Hz s^{-3})	–	*−12.4(3)*	*1.5(3)*	–	–	–
rms (phase)	0.0143	*0.1184*	*0.0210*	0.0160	0.0230	0.0226
χ^2/DOF	16/15	*1508.6/21*	*37.8/19*	19.1/19	46.6/25	40.6/20

[a] Values in parentheses are the uncertainties in the last digits of their associated measurements.
[b] These spin parameters yield unacceptable fits to data but listed here to illustrate the inadequacy of the polynomial model.

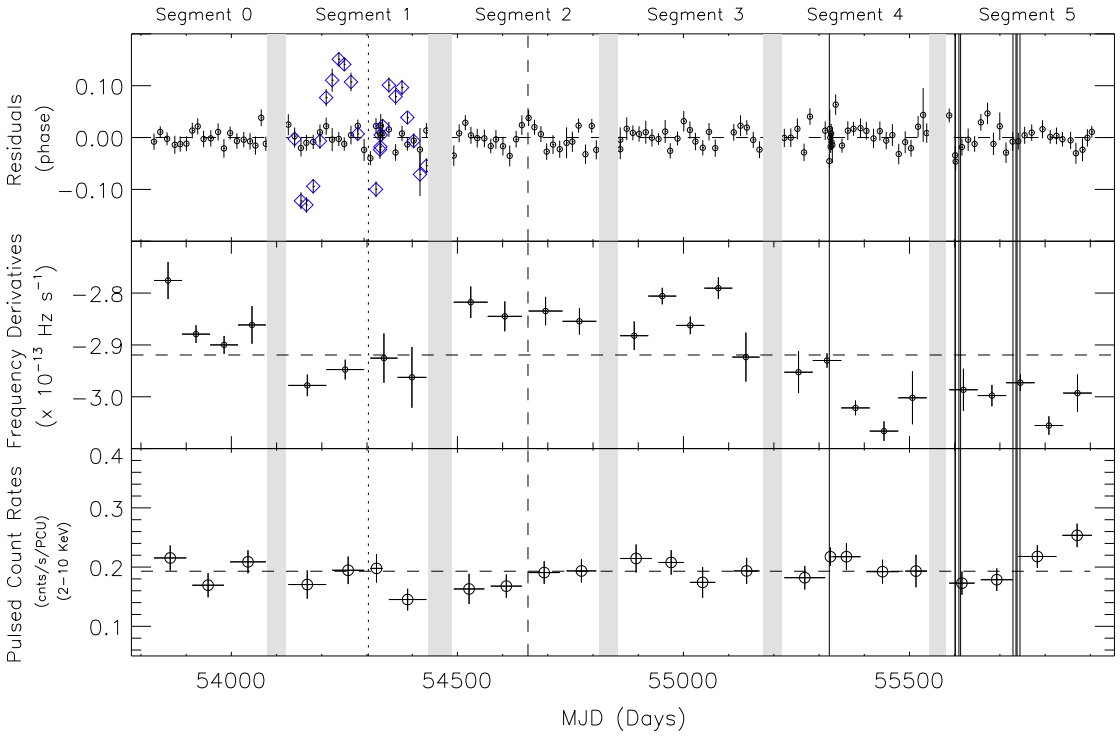

Figure 1. Top panel: phase residuals after the subtraction of the polynomial models presented in Table 1 from data. For Segment 1 we present the phase residuals after subtraction of the polynomial model (blue diamonds) presented in Table 1 and glitch model presented in Table 2 (See Figure 2 for more detailed presentation of this segment). Middle panel: frequency derivative evolution of the source. Bottom panel: evolution of the pulsed count rates in the 2−10 keV band. The times of glitch 4 and anti-glitch are shown with the vertical doted and dashed lines, respectively. The solid vertical lines indicate the times of energetic bursts listed in table 1 of Lin et al. (2011). Data gaps are indicated with light grey bars.

(Markwardt 2009) with a model involving a quadratic polynomial and a sudden change of spin frequency (i.e., glitch). The corresponding spin trend of this model is:

$$\nu(t) = \nu_0(t) + \Delta\nu + \Delta\dot{\nu}(t - t_g) \quad (2)$$

Here t_g is the time of the glitch. $\Delta\nu$ is the change in the frequency at the time of the glitch. $\Delta\dot{\nu}$ is the frequency derivative change after the glitch and $\nu_0(t)$ is pre-glitch frequency evolution.

In Segment 1, we found that a model involving a glitch provides statistically significant improvement in fitting the phase shifts (χ^2/DOF = 31.6/21). We, therefore, conclude that there is a glitch at MJD ∼54303 with an amplitude of $\Delta\nu$ ∼4×10^{-7} Hz. This is the 4th glitch observed from 1E 1841-045. We present the parameters for Glitch 4 in Table 2. Note that the amplitude of this glitch is on the order of last two glitches observed from this source (see Dib et al. 2008). We also present the phase residuals of the polynomial model and glitch model for comparison in Figure 2.

As we noted earlier, pulse phase modeling of the Segment 2 with a fourth order polynomial yields an unacceptable fit statistics (see panel c of Figure 3), while increasing

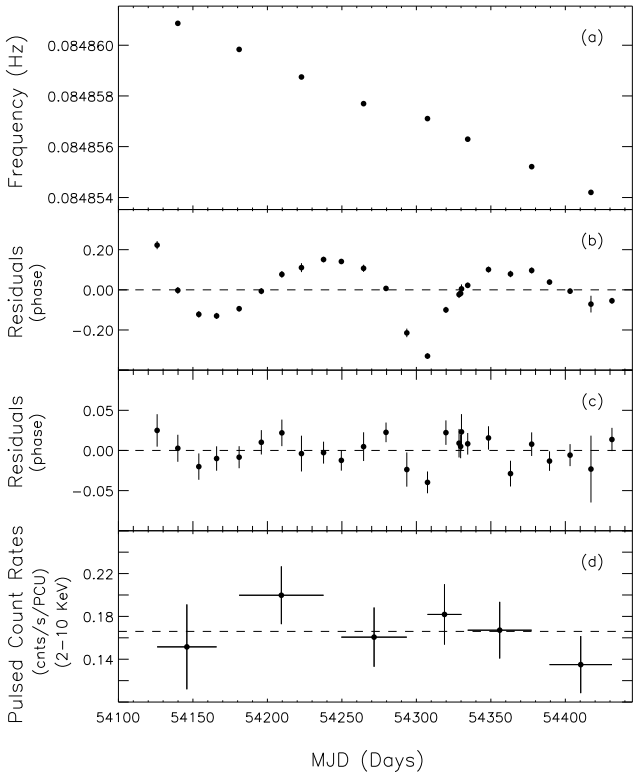

Figure 2. (a) Spin frequency evolution of the source during Segment 1. (b) Phase residuals after the subtraction of a fourth order polynomial model from the data. (c) Phase residuals after subtracting the glitch model. (d) Pulsed count rates of the source in the 2−10 keV band obtained using sets of observations spanning mostly over 40−50 d to ensure significant pulsed flux measurement.

Table 2. Parameters for Glitch 4[a]

Range (MJD)	54126−54431
Epoch (MJD)	54125.967
Number of TOAs	26
ν (Hz)	0.084861236(2)
$\dot{\nu}$ (10^{-13} Hz s^{-1})	−2.965(3)
t_g (MJD)	54303(3)
$\Delta\nu$ (10^{-8} Hz)	40.7(6)
$\Delta\dot{\nu}$ (10^{-15} Hz s^{-1})	1.2(7)
rms (phase)	0.0174
χ^2/DOF	31.6/21

[a] Values in parentheses are the uncertainties in the last digits of their associated measurements.

the order of polynomial results in unconstrained spin parameters. For this reason, we also modeled the phases of this segment with a glitch model. We find that an ordinary glitch model fit does not improve the fit statistics. However, a glitch with a negative amplitude (i.e., an anti-glitch) of $\Delta\nu \sim -5\times10^{-8}$ Hz provides a significant improvement in fit statistics (χ^2/DOF = 16.3/19); a $\Delta\chi^2$ of 21.5 for the same number of DOF as the polynomial model fit. Based on this, we conclude that 1E 1841-045 exhibited an anti-glitch near MJD 54656, that is ∼1 yr after Glitch 4. We list the parameters of the anti-glitch model fit in Table 3. Note that fit

Table 3. Parameters for Anti-glitch[a]

Range (MJD)	54492−54807
Epoch (MJD)	54491.992
Number of TOAs	24
ν (Hz)	0.084852317(2)
$\dot{\nu}$ (10^{-13} Hz s^{-1})	−2.833(3)
t_g (MJD)	54656.0
$\Delta\nu$ (10^{-8} Hz)	−4.9(6)
$\Delta\dot{\nu}$ (10^{-15} Hz s^{-1})	−1.8(6)
rms (phase)	0.0139
χ^2/DOF	16.3/19

[a] Values in parentheses are the uncertainties in the last digits of their associated measurements.

results suggesting the anti-glitch epoch between MJD 54645 and 54662 yield similar fit statistics, indicating that the anti-glitch occurred in this time interval. In the top panel of Figure 3 we present the frequency evolution of the source in this segment. To show the sudden deviation of the spin frequency, we fit a linear trend to the frequencies prior to MJD ∼54650 and extrapolated this fit to the rest of this segment (see panel b in Figure 3). We found that the spin-down rate before MJD 54630 and after MJD 54670 are consistent with one another ($-2.84(1)\times10^{-13}$ and $-2.86(1)\times10^{-13}$ Hz s^{-1}, respectively). The average spin-down rate during the ∼40 d in between is about -3×10^{-13} Hz s^{-1}. We also present the phase residuals of the anti-glitch involving model in the panel d of Figure 3.

Fits to the pulse arrival times of Segment 4 and 5 with models involving a glitch or anti-glitch did not yield any improvement in the fit statistics. We therefore conclude that the system exhibits higher level of timing noise, likely related to the emission of numerous energetic bursts during these episodes (see Figure 1).

Finally, in order to search for radiative variabilities we performed pulsed count rate analysis as explained in Şaşmaz Muş & Göğüş (2013). We found that pulsed count rate of the source is constant over ∼5.5 yr of *RXTE* observations (See, third panel of Figure 1).

4 DISCUSSION AND CONCLUSIONS

1E 1841-045 was observed ∼13 yr by *RXTE*. Here we performed timing analysis of 1E 1841-045 using ∼5 yr of *RXTE* observations. Previous ∼7.6 yr has been analysed by (Dib et al. 2008) and 3 glitches have been reported. The largest glitch observed from this source has an amplitude of $\sim1.2\times10^{-6}$ Hz with a recovery timescale of 43 days and fractional increase of 0.1 in its spin-down rate. Consequent two glitches have amplitudes on the order of $\sim10^{-7}$ Hz without any observable exponential recovery. There is no evidence of accompanying radiative enhancements during all three glitch epochs.

Through our detailed investigations of *RXTE* monitoring of 1E 1841-045 spanning over five years, we have identified two timing events separated by ∼1 yr: a glitch and an 'anti-glitch'. The glitch event has occurred at MJD ∼54303 with an amplitude of $\Delta\nu\sim4\times10^{-7}$ Hz without any observable exponential recovery. Note that this is the fourth glitch identified from this source: one of the earlier three has an

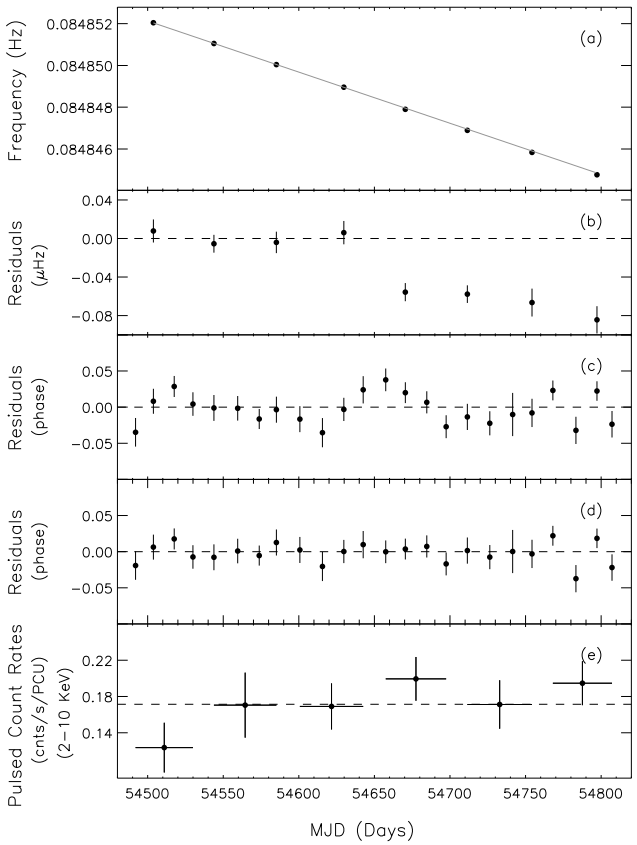

Figure 3. (a) Spin frequency evolution of the source during Segment 2. The solid line is the spin-down trend obtained by fitting the observations before MJD ∼54630, and extrapolated onwards. (b) Residuals of the model and its extrapolation in (a). (c) Phase residuals after the subtraction of a fourth order polynomial fit presented in Table 1. (d) Phase residuals after the subtraction the glitch model presented in Table 3 (e) The pulsed count rates in 2−10 keV averaged over ∼40 d.

amplitude of $\sim 10^{-6}$ Hz with a recovery timescale of 43 days (Dib et al. 2008), while the other two were at similar amplitudes and showed no exponential recovery. Similar to the three earlier glitch episodes in 1E 1841-045 , we found no associated radiative enhancement deduced from the pulsed X-ray flux measurement (bottom panels of Figure 1 and 2).

The second event, an anti-glitch seen from 1E 1841-045 for the first time, has occurred at MJD ∼54656 with an amplitude of $\Delta\nu \sim -5\times10^{-8}$ Hz. The amplitude of the only other anti-glitch event observed from 1E 2259+586 (Archibald et al. 2013a) is strikingly similar. We found that the source experienced an elevated spin-down rate over about 40 days, and $\dot{\nu}$ returned back to the pre-anti-glitch level after MJD 54670. Note that the average spin-down rate in the elevated regime is about -3×10^{-13} Hz s^{-1}, which is similar to the $\dot{\nu}$ values exhibited by the source over ∼150 d following an energetic burst on MJD 55322.6 (see the middle panel of Figure 1). Both pulsed X-ray emission (see the bottom panel of Figure 3) and the 0.5-10 keV flux (see figure 3 of Lin et al. 2011) of the source remain constant during the anti-glitch episode, similar to the case for the fourth glitch.

According to the standard pulsar glitch models (see for example Anderson & Itoh 1975; Alpar 1977), a faster rotating superfluid transfers angular momentum to the crust which results in positive increment in the observed spin frequency of the neutron star. Alpar & Baykal (1994) statistically determined that superfluid vortex unpinning model with a constant fractional vortex density, which is the fraction of vortex density involved in the glitch event, provides the most plausible explanation for glitches observed from rotation powered pulsars. In this model, the number of glitches in a given time span that a pulsar would experience is related to the constant fractional vortex density, the ratio of the spin-down rate and frequency of the pulsar. From previous observations and glitches observed from 1E 1841-045 we determined the fractional vortex density as 2.90×10^{-4}. Note that this is consistent with fractional vortex density for 1RXS J170849.0-400910 (Şaşmaz Muş & Göğüş 2013). Using this parameter for 1E 1841-045 and an average value of the ratio of the spin-down rate to the frequency yield the expected number of glitches from this magnetar during the entire 13 yr of *RXTE* observation span as 4.5. With the fourth glitch we uncovered in this study, our results are in agreement with the expectations of the vortex unpinning model.

Recent observation of the anti-glitch from 1E 2259+586 implies a neutron star superfluid interior rotating slower than the crust within the context of standard pulsar glitch models (Archibald et al. 2013a; Anderson & Itoh 1975). It was suggested that the rotation of the superfluid can be slowed down by crustal deformations due to magnetic stresses in highly magnetized sources Thompson et al. (2000); Duncan (2013). Thompson et al. (2000) suggest that 1E 2259+586 and 1E 1841-045 might have had episodes of accelerated spin-down due to the fact that they are older than their associated supernovae remnants as inferred by their characteristic ages. In Thompson et al. (2000) they also propose a particle outflow scheme to account for the sudden spin-down behaviour of SGR 1900+14[3] (Woods et al. 1999), in conjunction with its August 27 giant flare. However, there was no indication of particle outflow from 1E 2259+586 around the time of the anti-glitch (Archibald et al. 2013a). For this reason, the particle outflow scenario was discarded. Alternatively, there are already a couple of magnetospheric models suggested to understand the origin of the anti-glitch: Lyutikov (2013) proposed that the sudden spin-down and in general variable spin-down trends are caused by the changes in torque due to transient opening of a small region of the twisted magnetosphere during the X-ray burst. Tong et al. (2013); Tong (2014) have applied the wind braking scenario (Michel 1969; Harding et al. 1999; Thompson et al. 2000) to magnetars in the case that the rotational energy of the star is mainly extracted via a constant particle wind from the star. In this model an anti-glitch corresponds to an enhanced state of the particle wind (Tong 2014). Both partial magnetospheric opening and wind breaking models require radiative enhancements accompanying the anti-glitch, which was the case for 1E 2259+586 as

[3] The rapid spin-down trend in SGR 1900+14 can be considered as the first observational manifestation of an anti-glitch, though the sparsity of observations did not allow the firm confirmation.

its X-ray flux increased by at least a factor of two in association with the anti-glitch Archibald et al. (2013a). Our results, however, place an indirect constraint on both models since we found no observable variations in the pulsed X-ray emission from 1E 1841-045 at the time of its anti-glitch. Nevertheless, occasional detection of energetic bursts from 1E 1841-045 indicate that its magnetosphere is active and not all but some X-ray bursts may lead to a magnetospheric rearrangement that could lead to the episodic rapid spin-down as prescribed by Lyutikov (2013).

Note the fact that we became aware of the paper by Dib & Kaspi (2014) during the review stage of our paper. They fit a very wide data segment (spanning more than 1200 d and including our suggested anti-glitch) with a fifth-order polynomial, and find an rms of 0.041, which is much larger than that for any other segment. Even with the fifth-order polynomial fit, large fluctuations in the phase residuals are clearly visible (see panel (c) around MJD 54600 of figure 1c in Dib & Kaspi (2014)). They make no emphasis on this significant timing anomaly, which we interpret as an anti-glitch.

ACKNOWLEDGEMENTS

We thank M. Ali Alpar for helpful comments. SŞM acknowledges support through the national graduate fellowship program of The Scientific and Technological Research Council of Turkey (TÜBİTAK).

REFERENCES

Alpar M. A., 1977, ApJ, 213, 527
Alpar M. A., Baykal A., 1994, MNRAS, 269, 849
Anderson P. W., Itoh N., 1975, Nature, 256, 25
Archibald R. et al., 2013a, Nature, 497, 591
Archibald R., Scholz P., Kaspi V. M., 2013b, ATel, 5420
Collazzi A. C., Xiong S., Kouveliotou C., 2013, GRB Coordinates Network, Circular Service, 15228
Dall'Osso S., Israel G. L., Stella L., Possenti A., Perozzi E., 2003, ApJ, 599, 485
Dib R., Kaspi V. M., 2014, preprint(arXiv:1401.3085v1)
Dib R., Kaspi V. M., Gavriil F. P., 2008, ApJ, 673, 1044
Dib R., Kaspi V. M., Gavriil F. P., 2009, ApJ, 702, 614
Duncan R. C., 2013, Nature, 497, 574
Duncan R. C., Thompson C., 1992, ApJ, 392, L9
Foley S., Kouveliotou C., Kaneko Y., Collazzi A., 2012, GRB Coordinates Network, Circular Service, 13280, 1
Gavriil F. P., Kaspi V. M., Woods P. M., 2002, Nature, 419, 142
Gavriil F. P., Kaspi V. M., Woods P. M., 2006, ApJ, 641, 418
Gavriil F. P., Dib R., Kaspi V. M., 2011, ApJ, 736, 138
Harding A. K., Contopoulos I., Kazanas D., 1999, ApJ, 525, L125
Hu Y., Pitkin M., Heng I. S., Hendry M. A., 2014, ApJ, 784, L41
Huang Y. F., Geng J. J., 2014, ApJ, 782, L20
Israel G. L., Götz D., Zane S., Dall'Osso S., Rea N., Stella L., 2007a, A&A, 476, L9
Israel G. L., Campana S., Dall'Osso S., Muno M. P., Cummings J., Perna R., Stella L., 2007b, ApJ, 664, 448
Jahoda K., Markwardt C. M., Radeva Y., Rots A. H., Stark M. J., Swank J. H., Strohmayer T. E., Zhang W., 2006, ApJS, 163, 401
Kaspi V. M., Gavriil F. P., 2003b, ApJ, 596, L71
Kaspi V. M., Lackey J. R., Chakrabarty D., 2000, ApJ, 537, L31
Kaspi V. M., Gavriil F. P., Woods P. M., Jensen J. B., Roberts M. S. E., Chakrabarty D., 2003a, ApJ, 588, L96
Katz J. I., 2014, Ap&SS, 349, 611
Krimm H., Barthelmy S., Campana S., Cummings J., Israel G., Palmer D., Parsons A., 2006, ATel, 894
Kuiper L., Hermsen W., Mendez, M., 2004, ApJ, 613, 1173
Kumar H. S., Safi-Harb S., 2010, ApJ, 725, L191
Lin L. et al., 2011, ApJ, 740, L16
Lyutikov M., 2013, preprint(arXiv:1306.2264v1)
Markwardt C. B., 2009, in Bohlender D., Dowler P., durand D., eds, ASP Conf. Ser. Vol. 411, Astronomical Data Analysis Software and Systems XVIII. Astron. Soc. Pac., San Francisco, p. 251
Mereghetti S., 2011, Advances in Space Research, 47, 1317
Michel F. C., 1969, ApJ, 158, 727
Muno M. P., Gaensler B. M., Clark J. S., de Grijs R., Pooley D., Stevens I. R., Portegies Zwart S. F., 2007, MNRAS, 378, L44
Ouyed R., Leahy D., Koning N., 2013, preprint(arXiv:1307.1386v1)
Pal'shin V. et al., 2013, GRB Coordinates Network, Circular Service, 15245
Rea N., Esposito P., 2011, in "High Energy Emission from Pulsars and their Systems", D. F. Torres & N. Rea, ed., (Berlin: Springer), 247
Şaşmaz Muş S., Göğüş E., 2013, ApJ, 778, 156
Tam R. C., Gavriil F. P., Dib R., Kaspi V. M., Woods P. M., Bassa C., 2008, ApJ, 677, 503
Thompson C., Duncan R. C., Woods P. M., Kouveliotou C., Finger M., van Paradijs J., 2000, ApJ, 543, 340
Tong H., 2014, ApJ, 677, 503
Tong H., Xu R. X, Song L. M., Qiao G. J., 2013a, ApJ, 768, 144
Woods P. M. et al., 1999, ApJ, 524, L55
Woods P. M. et al., 2004, ApJ, 605, 378
Woods P. M., Kaspi V. M., Gavriil F. P., Airhart C., 2011, ApJ, 726, 37
Zhu W., Kaspi V. M., 2010, ApJ, 719, 351